

EUROPEAN ORGANIZATION FOR NUCLEAR RESEARCH

CERN-PH-EP-2008-017

10 November 2008

Inclusive single-particle production in two-photon collisions at LEP II with the DELPHI detector

DELPHI Collaboration

Abstract

A study of the inclusive charged hadron production in two-photon collisions is described. The data were collected with the DELPHI detector at LEP II. Results on the inclusive single-particle p_T distribution and the differential charged hadrons $d\sigma/dp_T$ cross-section are presented and compared to the predictions of perturbative NLO QCD calculations and to published results.

(Accepted by Phys. Lett. B)

J.Abdallah²⁷, P.Abreu²⁴, W.Adam⁵⁶, P.Adzic¹³, T.Albrecht¹⁹, R.Aleman-Fernandez¹⁰, T.Allmendinger¹⁹,
 P.P.Allport²⁵, U.Amaldi³¹, N.Amapane⁴⁹, S.Amato⁵³, E.Anashkin³⁸, A.Andreaazza³⁰, S.Andringa²⁴, N.Anjos²⁴,
 P.Antilogus²⁷, W-D.Apel¹⁹, Y.Arnoud¹⁶, S.Ask¹⁰, B.Asman⁴⁸, J.E.Augustin²⁷, A.Augustinus¹⁰, P.Baillon¹⁰,
 A.Ballestrero⁵⁰, P.Bambade²², R.Barbier²⁹, D.Bardin¹⁸, G.J.Barker⁵⁸, A.Baroncelli⁴¹, M.Battaglia¹⁰, M.Baubillier²⁷,
 K-H.Becks⁵⁹, M.Begalli⁸, A.Behrmann⁵⁹, E.Ben-Haim²², N.Benekos³⁴, A.Benvenuti⁶, C.Berat¹⁶, M.Berggren²⁷,
 D.Bertrand³, M.Besancon⁴², N.Besson⁴², D.Bloch¹¹, M.Blom³³, M.Bluj⁵⁷, M.Bonesini³¹, M.Boonekamp⁴²,
 P.S.L.Booth^{†25}, G.Borisov²³, O.Botner⁵⁴, B.Bouquet²², T.J.V.Bowcock²⁵, I.Boyko¹⁸, M.Bracko⁴⁵, R.Brenner⁵⁴,
 E.Brodet³⁷, P.Bruckman²⁰, J.M.Brunet⁹, B.Buschbeck⁵⁶, P.Buschmann⁵⁹, M.Calvi³¹, T.Camporesi¹⁰, V.Canale⁴⁰,
 F.Carena¹⁰, N.Castro²⁴, F.Cavallo⁶, M.Chapkin⁴⁴, Ph.Charpentier¹⁰, P.Checchia³⁸, R.Chierici¹⁰, P.Chliapnikov⁴⁴,
 J.Chudoba¹⁰, S.U.Chung¹⁰, K.Cieslik²⁰, P.Collins¹⁰, R.Contri¹⁵, G.Cosme²², F.Cossutti⁵¹, M.J.Costa⁵⁵, D.Crennell³⁹,
 J.Cuevas³⁶, J.D'Hondt³, T.da Silva⁵³, W.Da Silva²⁷, G.Della Ricca⁵¹, A.De Angelis⁵², W.De Boer¹⁹, C.De Clercq³,
 B.De Lotto⁵², N.De Maria⁴⁹, A.De Min³⁸, L.de Paula⁵³, L.Di Ciaccio⁴⁰, A.Di Simone⁴¹, K.Doroba⁵⁷, J.Drees^{59,10},
 G.Eigen⁵, T.Ekelof⁵⁴, M.Ellert⁵⁴, M.Elsing¹⁰, M.C.Espirito Santo²⁴, G.Fanourakis¹³, D.Fassouliotis^{13,4}, M.Feindt¹⁹,
 J.Fernandez⁴³, A.Ferrer⁵⁵, F.Ferro¹⁵, U.Flagmeyer⁵⁹, H.Foeth¹⁰, E.Fokitis³⁴, F.Fulda-Quenzer²², J.Fuster⁵⁵,
 M.Gandelman⁵³, C.Garcia⁵⁵, Ph.Gavillet¹⁰, E.Gazis³⁴, R.Gokieli^{10,57}, B.Golob^{45,47}, G.Gomez-Ceballos⁴³,
 P.Goncalves²⁴, E.Graziani⁴¹, G.Grosdidier²², K.Grzelak⁵⁷, J.Guy³⁹, C.Haag¹⁹, A.Hallgren⁵⁴, K.Hamacher⁵⁹,
 K.Hamilton³⁷, S.Haug³⁵, F.Hauler¹⁹, V.Hedberg²⁸, M.Hennecke¹⁹, J.Hoffman⁵⁷, S-O.Holmgren⁴⁸, P.J.Holt¹⁰,
 M.A.Houlden²⁵, J.N.Jackson²⁵, G.Jarlskog²⁸, P.Jarry⁴², D.Jeans³⁷, E.K.Johansson⁴⁸, P.Jonsson²⁹, C.Joram¹⁰,
 L.Jungermann¹⁹, F.Kapusta²⁷, S.Katsanevas²⁹, E.Katsoufis³⁴, G.Kernel⁴⁵, B.P.Kersevan^{45,47}, U.Kerzel¹⁹, B.T.King²⁵,
 N.J.Kjaer¹⁰, P.Kluit³³, P.Kokkinias¹³, C.Kourkouvelis⁴, O.Kouznetsov¹⁸, Z.Krumstein¹⁸, M.Kucharczyk²⁰, J.Lamsa¹,
 G.Leder⁵⁶, F.Ledroit¹⁶, L.Leinonen⁴⁸, R.Leitner³², J.Lemonne³, V.Lepeltier^{†22}, T.Lesiak²⁰, W.Liebig⁵⁹, D.Liko⁵⁶,
 A.Lipniacka⁴⁸, J.H.Lopes⁵³, J.M.Lopez³⁶, D.Loukas¹³, P.Lutz⁴², L.Lyons³⁷, J.MacNaughton⁵⁶, A.Malek⁵⁹, S.Maltesos³⁴,
 F.Mandl⁵⁶, J.Marco⁴³, R.Marco⁴³, B.Marechal⁵³, M.Margoni³⁸, J-C.Marin¹⁰, C.Mariotti¹⁰, A.Markou¹³,
 C.Martinez-Rivero⁴³, J.Masik¹⁴, N.Mastroyiannopoulos¹³, F.Matorras⁴³, C.Matteuzzi³¹, F.Mazzucato³⁸,
 M.Mazzucato³⁸, R.Mc Nulty²⁵, C.Meroni³⁰, E.Migliore⁴⁹, W.Mitaroff⁵⁶, U.Mjoernmark²⁸, T.Moa⁴⁸, M.Moch¹⁹,
 K.Moenig^{10,12}, R.Monge¹⁵, J.Montenegro³³, D.Moraes⁵³, S.Moreno²⁴, P.Morettini¹⁵, U.Mueller⁵⁹, K.Muenich⁵⁹,
 M.Mulders³³, L.Mundim⁸, W.Murray³⁹, B.Muryn²¹, G.Myatt³⁷, T.Myklebust³⁵, M.Nassiakou¹³, F.Navarria⁶,
 K.Nawrocki⁵⁷, S.Nemecek¹⁴, R.Nicolaidou⁴², M.Nikolenko^{18,11}, A.Oblakowska-Mucha²¹, V.Obraztsov⁴⁴, A.Olshevski¹⁸,
 A.Onofre²⁴, R.Orava¹⁷, K.Osterberg¹⁷, A.Ouraou⁴², A.Oyanguren⁵⁵, M.Paganoni³¹, S.Paiano⁶, J.P.Palacios²⁵,
 H.Palka²⁰, Th.D.Papadopoulou³⁴, L.Pape¹⁰, C.Parkes²⁶, F.Parodi¹⁵, U.Parzefall¹⁰, A.Passerini⁴¹, O.Passon⁵⁹,
 L.Peralta²⁴, V.Perepelitsa⁵⁵, A.Perrotta⁶, A.Petrolini¹⁵, J.Piedra⁴³, L.Pieri⁴¹, F.Pierre⁴², M.Pimenta²⁴, E.Piotto¹⁰,
 T.Podobnik^{45,47}, V.Poireau¹⁰, M.E.Pol⁷, G.Polok²⁰, V.Pozdniakov¹⁸, N.Pukhaeva¹⁸, A.Pullia³¹, D.Radojicic³⁷,
 P.Rebecchi¹⁰, J.Rehn¹⁹, D.Reid³³, R.Reinhardt⁵⁹, P.Renton³⁷, F.Richard²², J.Ridky¹⁴, M.Rivero⁴³, D.Rodriguez⁴³,
 A.Romero⁴⁹, P.Ronchese³⁸, P.Roudeau²², T.Rovelli⁶, V.Ruhlmann-Kleider⁴², D.Ryabtchikov⁴⁴, A.Sadovsky¹⁸,
 L.Salmi¹⁷, J.Salt⁵⁵, C.Sander¹⁹, A.Savoy-Navarro²⁷, U.Schwickerath¹⁰, R.Sekulin³⁹, M.Siebel⁵⁹, A.Sisakian¹⁸,
 G.Smadja²⁹, O.Smirnova²⁸, A.Sokolov⁴⁴, A.Sopczak²³, R.Sosnowski⁵⁷, T.Spassov¹⁰, M.Stanitzki¹⁹, A.Stocchi²²,
 J.Strauss⁵⁶, B.Stugu⁵, M.Szczekowski⁵⁷, M.Szeptycka⁵⁷, T.Szumlak²¹, T.Tabarelli³¹, F.Tegenfeldt⁵⁴, J.Timmermans³³,
 L.Tkatchev¹⁸, M.Tobin²⁵, S.Todorovova¹⁴, B.Tome²⁴, A.Tonazzo³¹, P.Tortosa⁵⁵, P.Travnicek¹⁴, D.Treille¹⁰,
 G.Tristram⁹, M.Trochimczuk⁵⁷, C.Troncon³⁰, M-L.Turluer⁴², I.A.Tyapkin¹⁸, P.Tyapkin¹⁸, S.Tzamarias¹³, V.Uvarov⁴⁴,
 G.Valenti⁶, P.Van Dam³³, J.Van Eldik¹⁰, N.van Remortel², I.Van Vulpen¹⁰, G.Vegni³⁰, F.Veloso²⁴, W.Venus³⁹,
 P.Verdier²⁹, V.Verzi⁴⁰, D.Vilanova⁴², L.Vitale⁵¹, V.Vrba¹⁴, H.Wahlen⁵⁹, A.J.Washbrook²⁵, C.Weiser¹⁹, D.Wicke¹⁰,
 J.Wickens³, G.Wilkinson³⁷, M.Winter¹¹, M.Witek²⁰, O.Yushchenko⁴⁴, A.Zalewska²⁰, P.Zalewski⁵⁷, D.Zavrtanik⁴⁶,
 V.Zhuravlov¹⁸, N.I.Zimin¹⁸, A.Zintchenko¹⁸, M.Zupan¹³

-
- ¹Department of Physics and Astronomy, Iowa State University, Ames IA 50011-3160, USA
²Physics Department, Universiteit Antwerpen, Universiteitsplein 1, B-2610 Antwerpen, Belgium
³IIHE, ULB-VUB, Pleinlaan 2, B-1050 Brussels, Belgium
⁴Physics Laboratory, University of Athens, Solonos Str. 104, GR-10680 Athens, Greece
⁵Department of Physics, University of Bergen, Allégaten 55, NO-5007 Bergen, Norway
⁶Dipartimento di Fisica, Università di Bologna and INFN, Viale C. Berti Pichat 6/2, IT-40127 Bologna, Italy
⁷Centro Brasileiro de Pesquisas Físicas, rua Xavier Sigaud 150, BR-22290 Rio de Janeiro, Brazil
⁸Inst. de Física, Univ. Estadual do Rio de Janeiro, rua São Francisco Xavier 524, Rio de Janeiro, Brazil
⁹Collège de France, Lab. de Physique Corpusculaire, IN2P3-CNRS, FR-75231 Paris Cedex 05, France
¹⁰CERN, CH-1211 Geneva 23, Switzerland
¹¹Institut de Recherches Subatomiques, IN2P3 - CNRS/ULP - BP20, FR-67037 Strasbourg Cedex, France
¹²Now at DESY-Zeuthen, Platanenallee 6, D-15735 Zeuthen, Germany
¹³Institute of Nuclear Physics, N.C.S.R. Demokritos, P.O. Box 60228, GR-15310 Athens, Greece
¹⁴FZU, Inst. of Phys. of the C.A.S. High Energy Physics Division, Na Slovance 2, CZ-182 21, Praha 8, Czech Republic
¹⁵Dipartimento di Fisica, Università di Genova and INFN, Via Dodecaneso 33, IT-16146 Genova, Italy
¹⁶Institut des Sciences Nucléaires, IN2P3-CNRS, Université de Grenoble 1, FR-38026 Grenoble Cedex, France
¹⁷Helsinki Institute of Physics and Department of Physical Sciences, P.O. Box 64, FIN-00014 University of Helsinki, Finland
¹⁸Joint Institute for Nuclear Research, Dubna, Head Post Office, P.O. Box 79, RU-101 000 Moscow, Russian Federation
¹⁹Institut für Experimentelle Kernphysik, Universität Karlsruhe, Postfach 6980, DE-76128 Karlsruhe, Germany
²⁰Institute of Nuclear Physics PAN, Ul. Radzikowskiego 152, PL-31142 Krakow, Poland
²¹Faculty of Physics and Nuclear Techniques, University of Mining and Metallurgy, PL-30055 Krakow, Poland
²²LAL, Univ Paris-Sud, CNRS/IN2P3, Orsay, France
²³School of Physics and Chemistry, University of Lancaster, Lancaster LA1 4YB, UK
²⁴LIP, IST, FCUL - Av. Elias Garcia, 14-1º, PT-1000 Lisboa Codex, Portugal
²⁵Department of Physics, University of Liverpool, P.O. Box 147, Liverpool L69 3BX, UK
²⁶Dept. of Physics and Astronomy, Kelvin Building, University of Glasgow, Glasgow G12 8QQ, UK
²⁷LPNHE, IN2P3-CNRS, Univ. Paris VI et VII, Tour 33 (RdC), 4 place Jussieu, FR-75252 Paris Cedex 05, France
²⁸Department of Physics, University of Lund, Sölvegatan 14, SE-223 63 Lund, Sweden
²⁹Université Claude Bernard de Lyon, IPNL, IN2P3-CNRS, FR-69622 Villeurbanne Cedex, France
³⁰Dipartimento di Fisica, Università di Milano and INFN-MILANO, Via Celoria 16, IT-20133 Milan, Italy
³¹Dipartimento di Fisica, Univ. di Milano-Bicocca and INFN-MILANO, Piazza della Scienza 3, IT-20126 Milan, Italy
³²IPNP of MFF, Charles Univ., Areal MFF, V Holesovickach 2, CZ-180 00, Praha 8, Czech Republic
³³NIKHEF, Postbus 41882, NL-1009 DB Amsterdam, The Netherlands
³⁴National Technical University, Physics Department, Zografou Campus, GR-15773 Athens, Greece
³⁵Physics Department, University of Oslo, Blindern, NO-0316 Oslo, Norway
³⁶Dpto. Fisica, Univ. Oviedo, Avda. Calvo Sotelo s/n, ES-33007 Oviedo, Spain
³⁷Department of Physics, University of Oxford, Keble Road, Oxford OX1 3RH, UK
³⁸Dipartimento di Fisica, Università di Padova and INFN, Via Marzolo 8, IT-35131 Padua, Italy
³⁹Rutherford Appleton Laboratory, Chilton, Didcot OX11 0QX, UK
⁴⁰Dipartimento di Fisica, Università di Roma II and INFN, Tor Vergata, IT-00173 Rome, Italy
⁴¹Dipartimento di Fisica, Università di Roma III and INFN, Via della Vasca Navale 84, IT-00146 Rome, Italy
⁴²DAPNIA/Service de Physique des Particules, CEA-Saclay, FR-91191 Gif-sur-Yvette Cedex, France
⁴³Instituto de Física de Cantabria (CSIC-UC), Avda. los Castros s/n, ES-39006 Santander, Spain
⁴⁴Inst. for High Energy Physics, Serpukov P.O. Box 35, Protvino, (Moscow Region), Russian Federation
⁴⁵J. Stefan Institute, Jamova 39, SI-1000 Ljubljana, Slovenia
⁴⁶Laboratory for Astroparticle Physics, University of Nova Gorica, Kostanjevska 16a, SI-5000 Nova Gorica, Slovenia
⁴⁷Department of Physics, University of Ljubljana, SI-1000 Ljubljana, Slovenia
⁴⁸Fysikum, Stockholm University, Box 6730, SE-113 85 Stockholm, Sweden
⁴⁹Dipartimento di Fisica Sperimentale, Università di Torino and INFN, Via P. Giuria 1, IT-10125 Turin, Italy
⁵⁰INFN, Sezione di Torino and Dipartimento di Fisica Teorica, Università di Torino, Via Giuria 1, IT-10125 Turin, Italy
⁵¹Dipartimento di Fisica, Università di Trieste and INFN, Via A. Valerio 2, IT-34127 Trieste, Italy
⁵²Istituto di Fisica, Università di Udine and INFN, IT-33100 Udine, Italy
⁵³Univ. Federal do Rio de Janeiro, C.P. 68528 Cidade Univ., Ilha do Fundão BR-21945-970 Rio de Janeiro, Brazil
⁵⁴Department of Radiation Sciences, University of Uppsala, P.O. Box 535, SE-751 21 Uppsala, Sweden
⁵⁵IFIC, Valencia-CSIC, and D.F.A.M.N., U. de Valencia, Avda. Dr. Moliner 50, ES-46100 Burjassot (Valencia), Spain
⁵⁶Institut für Hochenergiephysik, Österr. Akad. d. Wissensch., Nikolsdorfergasse 18, AT-1050 Vienna, Austria
⁵⁷Inst. Nuclear Studies and University of Warsaw, Ul. Hoza 69, PL-00681 Warsaw, Poland
⁵⁸Now at University of Warwick, Coventry CV4 7AL, UK
⁵⁹Fachbereich Physik, University of Wuppertal, Postfach 100 127, DE-42097 Wuppertal, Germany
† deceased

1 Introduction

The inclusive production of hadrons in $\gamma^*\gamma^*$ interactions can be used to study the structure of two-photon collisions [1]. These photons are radiated by beam electrons which scatter at very small angles and most of them are not detected. The untagged photons are quasi-real with a mass $Q^2 \sim 0$. At LEP II these collisions are the main source of hadron production, providing a good opportunity for such an investigation and thus to check the predictions of leading and next-to-leading order (NLO) perturbative QCD computations.

The L3 and OPAL collaborations have published results of their analyses of the inclusive production of charged hadrons in two-photon collisions [2,3]. While L3 observes a pion production cross-section largely exceeding the NLO QCD predictions at high transverse momenta ($5 \text{ GeV}/c < p_T < 17 \text{ GeV}/c$), OPAL finds a good agreement with them, in the $p_T < 10 \text{ GeV}/c$ range of its analysis.

In this paper we present the DELPHI study of the inclusive production of charged hadrons in collisions of quasi-real photons. Section 2 describes the selection criteria for the event sample collected for this study. The inclusive single-particle transverse momentum spectrum and the measurement of the differential charged hadrons cross-section are presented in Section 3. They are compared to theoretical QCD predictions and published results in Section 4.

2 Experimental procedure

The analysis presented here is based on the data taken with the DELPHI detector [4,5] in 1996-2000, covering a range of centre-of-mass energies from 161 GeV to 209 GeV, with a luminosity-weighted average centre-of-mass energy: 195.5 GeV. The selected data set corresponds to the period when the Time Projection Chamber (TPC), the main tracking device of DELPHI, was fully operational thus ensuring good particle reconstruction. The corresponding integrated luminosity used in this analysis is 617 pb^{-1} .

The charged particles were measured in the tracking system of DELPHI, which consists of the microVertex Detector (VD), the Inner Detector (ID), the TPC, the Outer Detector (OD) in the barrel, and the Forward Chambers FCA and FCB in the endcaps of DELPHI, all embedded in a homogeneous 1.2 T magnetic field. The following selection criteria are applied to charged particles :

- transverse momentum $p_T > 150 \text{ MeV}/c$;
- impact parameter of a trajectory transverse to the beam axis $\Delta_{xy} < 0.4 \text{ cm}$;
- impact parameter of a trajectory along the beam axis $\Delta_z < 2 \text{ cm}$;
- polar angle of a track with respect to the e^- beam $10^\circ < \theta < 170^\circ$;
- track length $l > 30 \text{ cm}$;
- relative error of its momentum $\Delta p/p < 100\%$.

The measurement of neutral particles is made using the calorimeter information provided by the electromagnetic calorimeters, the High Density Projection Chamber (HPC) in the barrel and Forward Electromagnetic Calorimeter (FEMC) in the forward (backward) regions and by the hadronic calorimeter (HAC). Events with photons tagged by the DELPHI luminometer (STIC), i.e. with high Q^2 values, have been rejected. The calorimeter clusters, which are not associated to charged particle tracks, are combined to form the signals from the neutral particles (γ , π^0 , K_L^0 , n). The following thresholds are set on the measured energy: 0.5 GeV for showers in the electromagnetic calorimeters and

2 GeV for showers in the hadronic calorimeter. Furthermore the polar angle of neutral tracks was required to be in the range $10^\circ < \theta < 170^\circ$.

To extract the hadronic events from the collisions of quasi-real photons the following cuts are applied:

- energy deposited in the DELPHI luminometer (STIC: $2.5^\circ < \theta_{STIC} < 9^\circ$) $E_{STIC} < 30$ GeV;
- number of charged-particle tracks $N_{ch} > 4$;
- visible invariant mass, calculated from the four-momentum vectors of the measured charged and neutral particles, assuming the pion mass for charged particles, $5 \text{ GeV}/c^2 < W_{vis} < 35 \text{ GeV}/c^2$.

The first condition eliminates the so-called single and double-tagged $\gamma^*\gamma^*$ events. The condition on the charged track multiplicity as well as the lower limit on W_{vis} reduce the background from $\gamma^*\gamma^* \rightarrow \tau^+\tau^-$ events. The upper limit on W_{vis} cuts down the background from the $e^+e^- \rightarrow q\bar{q}(\gamma)$, $e^+e^- \rightarrow \tau^+\tau^-$ and four-fermion processes. The comparison of the W_{vis} distributions (Fig. 1) for the data and the Monte Carlo (MC) generated samples of events, described below, illustrates the effects of the W_{vis} cuts.

About 910k events are selected after application of the above selection criteria.

3 Data Analysis and Results

Monte Carlo samples of the various final states present in the data were generated for comparison with these data. The simulation of the process $\gamma^*\gamma^* \rightarrow \text{hadrons}$ was based on PYTHIA 6.143 [6] in which the description of the hadron production encompasses the processes described by the Quark Parton Model (QPM) (direct process), the Vector Dominance Model (VDM) and the hard scattering of the hadronic constituents of quasi-real photons (resolved photon process). The MC sample of events used is 2.7 times larger than the data. The main background coming from the inclusive $e^+e^- \rightarrow q\bar{q}(\gamma)$ channel has been estimated from a PYTHIA 6.125 sample. The simulations of the $e^+e^- \rightarrow$ four-fermion, the $\gamma^*\gamma^* \rightarrow \tau^+\tau^-$ and of the $e^+e^- \rightarrow \tau^+\tau^-$ backgrounds were based on the EXCALIBUR [7], BDKRC [8] and KORALZ 4.2 [9] generators, respectively. The Monte Carlo generated events were then passed through the standard DELPHI detector simulation and reconstruction programs [5]. The same cuts were applied on the reconstructed MC events as on the data.

The dN/dp_T distribution of the charged particles of the selected events is presented in Fig. 2, for tracks with pseudo-rapidity $|\eta| < 1$ ($\eta = -\ln \tan(\theta/2)$)¹, i.e. well measured tracks including TPC information. The expected Monte Carlo generated contributions, normalized to the data integrated luminosity are also shown. The data are well reproduced by the sum of the simulated samples of events for $p_T > 1.6 \text{ GeV}/c$ and the $e^+e^- \rightarrow q\bar{q}(\gamma)$ channel is the main contributor for $p_T > 12 \text{ GeV}/c$. There is a lack of data at $p_T < 1.6 \text{ GeV}/c$, becoming substantial at $p_T < 1 \text{ GeV}/c$. This is caused by the trigger efficiency which was not accounted for in the Monte Carlo simulation and which is low for low p_T tracks and low multiplicities [10]. For this reason, the following comparison with theoretical predictions is presented for $p_T > 1.6 \text{ GeV}/c$ only.

The differential $d\sigma/dp_T$ cross-section distribution of the inclusive production of charged hadrons in the process $\gamma^*\gamma^* \rightarrow \text{hadrons}$ has been obtained by subtracting the background contributions from the experimental dN/dp_T data. The resulting distribution has been

¹The angular selection of tracks (Table 1 and Figs. 2-5) is expressed in terms of $|\eta|$ cuts for comparison with published results [2,3].

corrected, bin-by-bin, by a factor which is the inverse of the ratio of the numbers of reconstructed to generated tracks of $\gamma^*\gamma^* \rightarrow \text{hadrons}$ in Monte Carlo events. This ratio is of the order of 50-60% for $1.6 \text{ GeV}/c < p_T < 4 \text{ GeV}/c$ and drops to about 20% for $p_T > 10 \text{ GeV}/c$, the upper bound on W_{vis} being mainly responsible for the drop in efficiency on large p_T tracks. The $d\sigma/dp_T$ distribution is shown in Fig. 3 for different sets of selection criteria as described below. The PYTHIA prediction is also shown. It agrees very well with the data for $p_T > 1.6 \text{ GeV}/c$ up to large p_T values.

To study the systematic uncertainty coming from the selection criteria, we have varied them, in particular the W_{vis} upper limit and the track polar angle (θ) cuts. A smaller upper bound of W_{vis} has the advantage of minimizing the background contributions especially the $e^+e^- \rightarrow q\bar{q} (\gamma)$ one. Tracks at low polar angle are missing TPC measurements and are thus less well measured. On the other hand most contributing processes correspond to the emission of tracks peaked in the forward (backward) regions, in particular the $e^+e^- \rightarrow q\bar{q} (\gamma)$ and even more the $\gamma^*\gamma^* \rightarrow \text{hadrons}$ channels. Hence a tight (θ) cut can reduce significantly the number of selected charged-particle tracks (N_{ch}) of a given event and consequently its computed visible energy W_{vis} . Fig. 3 shows the $d\sigma/dp_T$ distributions, calculated using tracks with $|\eta| < 1.5$, for four sets of selection criteria varying the polar angle selection imposed on charged tracks and the cut on the visible invariant mass W_{vis} :

1. $10^\circ < \theta < 170^\circ$ ($|\eta| < 2.4$), $5 \text{ GeV}/c^2 < W_{vis} < 20 \text{ GeV}/c^2$;
2. $25^\circ < \theta < 155^\circ$ ($|\eta| < 1.5$), $5 \text{ GeV}/c^2 < W_{vis} < 20 \text{ GeV}/c^2$;
3. $10^\circ < \theta < 170^\circ$ ($|\eta| < 2.4$), $5 \text{ GeV}/c^2 < W_{vis} < 35 \text{ GeV}/c^2$;
4. $25^\circ < \theta < 155^\circ$ ($|\eta| < 1.5$), $5 \text{ GeV}/c^2 < W_{vis} < 35 \text{ GeV}/c^2$.

The spread of the measurements is relatively small for $p_T < 7\text{-}8 \text{ GeV}/c$ but increases for high p_T values where the $e^+e^- \rightarrow q\bar{q} (\gamma)$ dominates. The corresponding systematic uncertainty has been estimated as half of the spread of the four sets of measurements.

The other source of uncertainty comes from the Monte Carlo modelling. It has been estimated by comparing the PYTHIA and TWOGAM [11] predictions for the $\gamma^*\gamma^* \rightarrow \text{hadrons}$ processes and PYTHIA and HERWIG [12] predictions for the $e^+e^- \rightarrow q\bar{q} (\gamma)$ process. It was found that the relative difference on the efficiencies calculated from the various generators depends on p_T but never exceeds 10%. The corresponding uncertainty has been defined as half of the difference between two generator contributions. All systematic uncertainties have been added quadratically in Table 1.

Table 1 gives the values of $d\sigma/dp_T$ as a function of p_T , for the selection criteria described in section 2, the pseudo-rapidity ranges $|\eta| < 1$ and $|\eta| < 1.5$ and for $p_T > 1.6 \text{ GeV}/c$ where the event trigger efficiency is close to 100%. The first error is statistical and the second one is the overall systematic uncertainty. Fig. 4 shows the comparison of the $d\sigma/dp_T$ distribution for $|\eta| < 1.5$ with the NLO QCD prediction of [13]. The theoretical computation tends to be slightly lower than the measurements at high p_T values although staying compatible with them within errors.

4 Discussion of results

Our measurement of the $d\sigma/dp_T$ cross-section of the inclusive production of hadrons in $\gamma^*\gamma^*$ interactions appears to agree well with both PYTHIA and NLO QCD predictions.

The L3 experiment has performed a similar analysis [2] and has observed that the p_T spectrum of charged hadrons is slightly below the PYTHIA MC prediction while the derived $d\sigma/dp_T$ cross-section considerably exceeds the NLO QCD prediction at high p_T

values. We have repeated our analysis, adopting a “L3-like” set of selection criteria which, compared to ours, corresponds to a less tight W_{vis} cut ($W_{vis} < 78 \text{ GeV}/c^2$ instead of $35 \text{ GeV}/c^2$) and a higher threshold of the total number of particles including neutrals (5 instead of 4). The looser W_{vis} cut has the effect of increasing significantly the $e^+e^- \rightarrow q\bar{q} (\gamma)$ background (see Fig. 1) which now dominates at large p_T values. The resulting dN/dp_T spectrum of charged particles for the “L3-like” events is presented in Fig. 5 together with the contributing channels. One observes an excess of data over the PYTHIA MC prediction. This disagreement between MC and data is likely to come from charged particles of background channels as these are introduced in much larger quantities than charged particles from $\gamma^*\gamma^* \rightarrow \text{hadrons}$, when the W_{vis} cut is relaxed up to $78 \text{ GeV}/c^2$, as can be checked by comparing Fig. 5 with Fig. 2. It legitimates, *a posteriori*, our $W_{vis} < 35 \text{ GeV}/c^2$ cut to minimize the contamination of charged particles from background channels.

The OPAL experiment has measured the differential $d\sigma/dp_T$ cross-section of the inclusive production of charged hadrons [3] for different intervals of W , the hadronic invariant mass corrected for detector effects. In the $(10 \text{ GeV}/c^2 < W < 30 \text{ GeV}/c^2)$ interval, the cross-section is compatible with the NLO prediction.

5 Conclusions

The study of the inclusive charged hadron production in two-photon collisions has been carried out at the DELPHI detector at LEP II. Measurements of the inclusive single-particle p_T distribution and of the differential inclusive $d\sigma/dp_T$ cross-section have been extracted. The differential inclusive $d\sigma/dp_T$ cross-section is found to be compatible, within errors, with the PYTHIA and NLO QCD predictions up to high p_T , although systematic uncertainties limit the accuracy of the comparison in this region. It is shown that if cuts such as those used in [2] are applied, $q\bar{q}$ background dominates at large p_T , making it difficult to draw conclusions on two-photon processes.

Acknowledgements

We are greatly indebted to our technical collaborators, to the members of the CERN-SL Division for the excellent performance of the LEP collider, and to the funding agencies for their support in building and operating the DELPHI detector.

We acknowledge in particular the support of

Austrian Federal Ministry of Education, Science and Culture, GZ 616.364/2-III/2a/98,
FNRS-FWO, Flanders Institute to encourage scientific and technological research in the industry (IWT) and Belgian Federal Office for Scientific, Technical and Cultural affairs (OSTC), Belgium,

FINEP, CNPq, CAPES, FUJB and FAPERJ, Brazil,

Ministry of Education of the Czech Republic, project LC527,

Academy of Sciences of the Czech Republic, project AV0Z10100502,

Commission of the European Communities (DG XII),

Direction des Sciences de la Matière, CEA, France,

Bundesministerium für Bildung, Wissenschaft, Forschung und Technologie, Germany,

General Secretariat for Research and Technology, Greece,

National Science Foundation (NSF) and Foundation for Research on Matter (FOM),

The Netherlands,

Norwegian Research Council,
State Committee for Scientific Research, Poland, SPUB-M/CERN/PO3/DZ296/2000,
SPUB-M/CERN/PO3/DZ297/2000, 2P03B 104 19 and 2P03B 69 23(2002-2004),
FCT - Fundação para a Ciência e Tecnologia, Portugal,
Vedecka grantova agentura MS SR, Slovakia, Nr. 95/5195/134,
Ministry of Science and Technology of the Republic of Slovenia,
CICYT, Spain, AEN99-0950 and AEN99-0761,
The Swedish Research Council,
The Science and Technology Facilities Council, UK,
Department of Energy, USA, DE-FG02-01ER41155,
EEC RTN contract HPRN-CT-00292-2002.

References

- [1] P. Aurenche *et al.*, in *Physics at LEP2*, eds. G. Altarelli, T. Sjöstrand and F. Zwirner, CERN 96-01 (1996) 291.
- [2] P. Achard *et al.*, L3 Collab., Phys. Lett. **B554** (2003) 105.
- [3] K. Ackerstaff *et al.*, OPAL Collab., Eur. Phys. J. **C6** (1999) 253.
- [4] P. Aarnio *et al.*, DELPHI Collab., Nucl. Inst. Meth. **A303** (1991) 233.
- [5] P. Abreu *et al.*, DELPHI Collab., Nucl. Inst. Meth. **A378** (1996) 57.
- [6] T. Sjöstrand *et al.*, Comput. Phys. Comm. **135** (2001) 238.
- [7] F.A. Berends, R. Pittau, R. Kleiss, Comput. Phys. Comm. **85** (1995) 437.
- [8] F.A. Berends, P.H. Daverveldt, R. Kleiss, Comput. Phys. Comm. **40** (1986) 271.
- [9] S. Jadach, B.F.L. Ward, Z. Was, Comput. Phys. Comm. **79** (1994) 503.
- [10] A. Augustinus *et al.*, DELPHI Trigger Group, Nucl. Inst. Meth. **A515** (2003) 782.
- [11] T. Alderweireld *et al.*, in *Reports of the Working Groups on Precision Calculations for LEP2 Physics*, eds. S. Jadach, G. Passarino and R. Pittau, CERN 2000-009 (2000) 219.
- [12] G. Marchesini *et al.*, Comput. Phys. Comm. **67** (1992) 465.
- [13] J. Binnewies, B.A Kniehl, G. Kramer, Phys. Rev. **D53** (1996) 6110.

p_T , GeV/c	$\langle p_T \rangle$, GeV/c	$d\sigma/dp_T$, pb/GeV/c	
		$ \eta < 1$	$ \eta < 1.5$
1.6 - 2.0	1.76	$(2.36 \pm 0.02^{+0.88}_{-0.41}) \times 10^2$	$(3.00 \pm 0.02^{+0.42}_{-0.60}) \times 10^2$
2.0 - 2.4	2.17	$(8.98 \pm 0.11^{+3.24}_{-1.18}) \times 10^1$	$(1.15 \pm 0.01^{+0.09}_{-0.17}) \times 10^2$
2.4 - 2.8	2.58	$(4.05 \pm 0.07^{+1.30}_{-0.58}) \times 10^1$	$(5.23 \pm 0.08^{+0.27}_{-0.82}) \times 10^1$
2.8 - 3.2	2.98	$(2.10 \pm 0.05^{+0.82}_{-0.27}) \times 10^1$	$(2.66 \pm 0.06^{+0.30}_{-0.38}) \times 10^1$
3.2 - 3.6	3.38	$(1.24 \pm 0.04^{+0.44}_{-0.17}) \times 10^1$	$(1.61 \pm 0.05^{+0.05}_{-0.25}) \times 10^1$
3.6 - 4.0	3.78	$(7.31 \pm 0.34^{+2.92}_{-1.06})$	$(9.41 \pm 0.35^{+1.03}_{-1.69})$
4.0 - 4.4	4.18	$(4.29 \pm 0.26^{+2.07}_{-0.47})$	$(5.54 \pm 0.27^{+0.85}_{-0.54})$
4.4 - 4.8	4.59	$(2.95 \pm 0.22^{+1.36}_{-0.46})$	$(3.89 \pm 0.24^{+0.42}_{-0.47})$
4.8 - 5.2	4.99	$(2.22 \pm 0.19^{+1.05}_{-0.12})$	$(2.78 \pm 0.20^{+0.29}_{-0.10})$
5.2 - 5.6	5.39	$(1.33 \pm 0.16^{+0.62}_{-0.05})$	$(1.65 \pm 0.16^{+0.19}_{-0.06})$
5.6 - 6.0	5.79	$(1.36 \pm 0.17^{+0.41}_{-0.25})$	$(1.70 \pm 0.19^{+0.12}_{-0.24})$
6.0 - 6.4	6.19	$(9.70 \pm 1.42^{+4.04}_{-1.20}) \times 10^{-1}$	$(1.16 \pm 0.15^{+0.15}_{-0.14})$
6.4 - 6.8	6.59	$(4.57 \pm 1.01^{+3.26}_{-0.88}) \times 10^{-1}$	$(8.34 \pm 1.36^{+0.47}_{-2.66}) \times 10^{-1}$
6.8 - 7.2	6.98	$(5.44 \pm 1.11^{+5.96}_{-3.03}) \times 10^{-1}$	$(6.65 \pm 1.12^{+2.52}_{-2.90}) \times 10^{-1}$
7.2 - 7.6	7.38	$(5.13 \pm 1.04^{+1.18}_{-0.92}) \times 10^{-1}$	$(5.43 \pm 1.09^{+0.28}_{-0.23}) \times 10^{-1}$
7.6 - 8.0	7.78	$(2.93 \pm 0.91^{+1.70}_{-1.57}) \times 10^{-1}$	$(3.67 \pm 0.92^{+0.38}_{-1.42}) \times 10^{-1}$
8.0 - 9.0	8.44	$(1.56 \pm 0.68^{+3.48}_{-1.33}) \times 10^{-1}$	$(2.65 \pm 1.23^{+1.94}_{-2.30}) \times 10^{-1}$
9.0 - 10.0	9.47	$(1.08 \pm 0.59^{+1.76}_{-0.89}) \times 10^{-1}$	$(1.71 \pm 0.86^{+1.41}_{-1.30}) \times 10^{-1}$
10.0 - 12.0	10.87	$(0.53 \pm 0.22^{+1.68}_{-0.44}) \times 10^{-1}$	$(0.68 \pm 0.28^{+1.37}_{-0.49}) \times 10^{-1}$
12.0 - 16.0	13.53	$(0.16 \pm 0.05^{+0.26}_{-0.02}) \times 10^{-1}$	$(0.23 \pm 0.07^{+0.43}_{-0.14}) \times 10^{-1}$

Table 1: Differential inclusive $d\sigma/dp_T$ of charged particles produced in $\gamma^*\gamma^* \rightarrow \text{hadrons}$ collisions, for $|\eta| < 1$, $|\eta| < 1.5$ and $p_T > 1.6$ GeV/c. The first error is statistical, the second is the systematic uncertainty. The data are background subtracted and corrected for detector inefficiency and selection cuts.

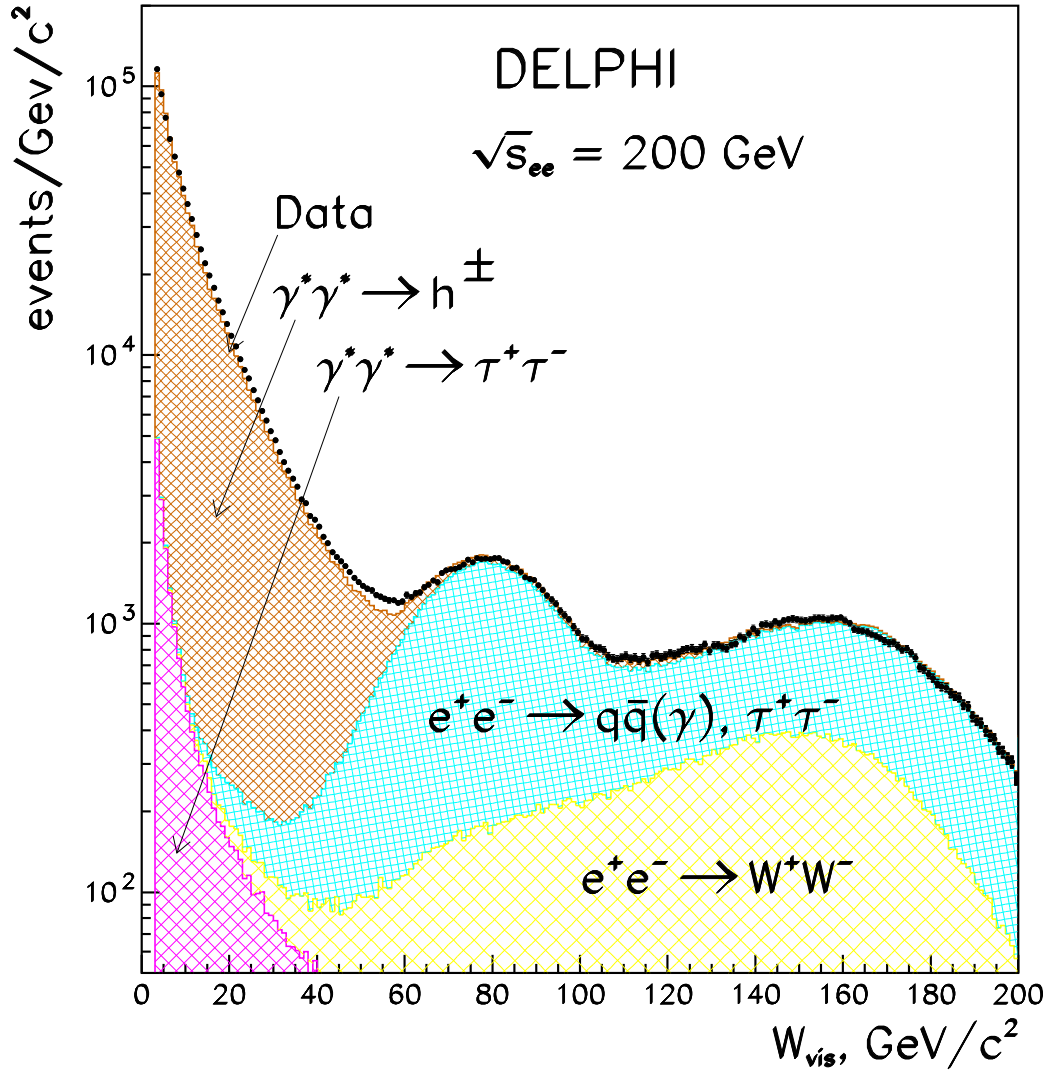


Figure 1: W_{vis} distributions for the data and for the simulated $\gamma^*\gamma^* \rightarrow \text{hadrons}$ (medium cross-hatching), $\gamma^*\gamma^* \rightarrow \tau^+\tau^-$ (second largest cross-hatching), $e^+e^- \rightarrow q\bar{q}(\gamma), \tau^+\tau^-$ (small cross-hatching) and $e^+e^- \rightarrow W^+W^-$ (largest cross-hatching) events at $\sqrt{s_{ee}} = 200 \text{ GeV}$.

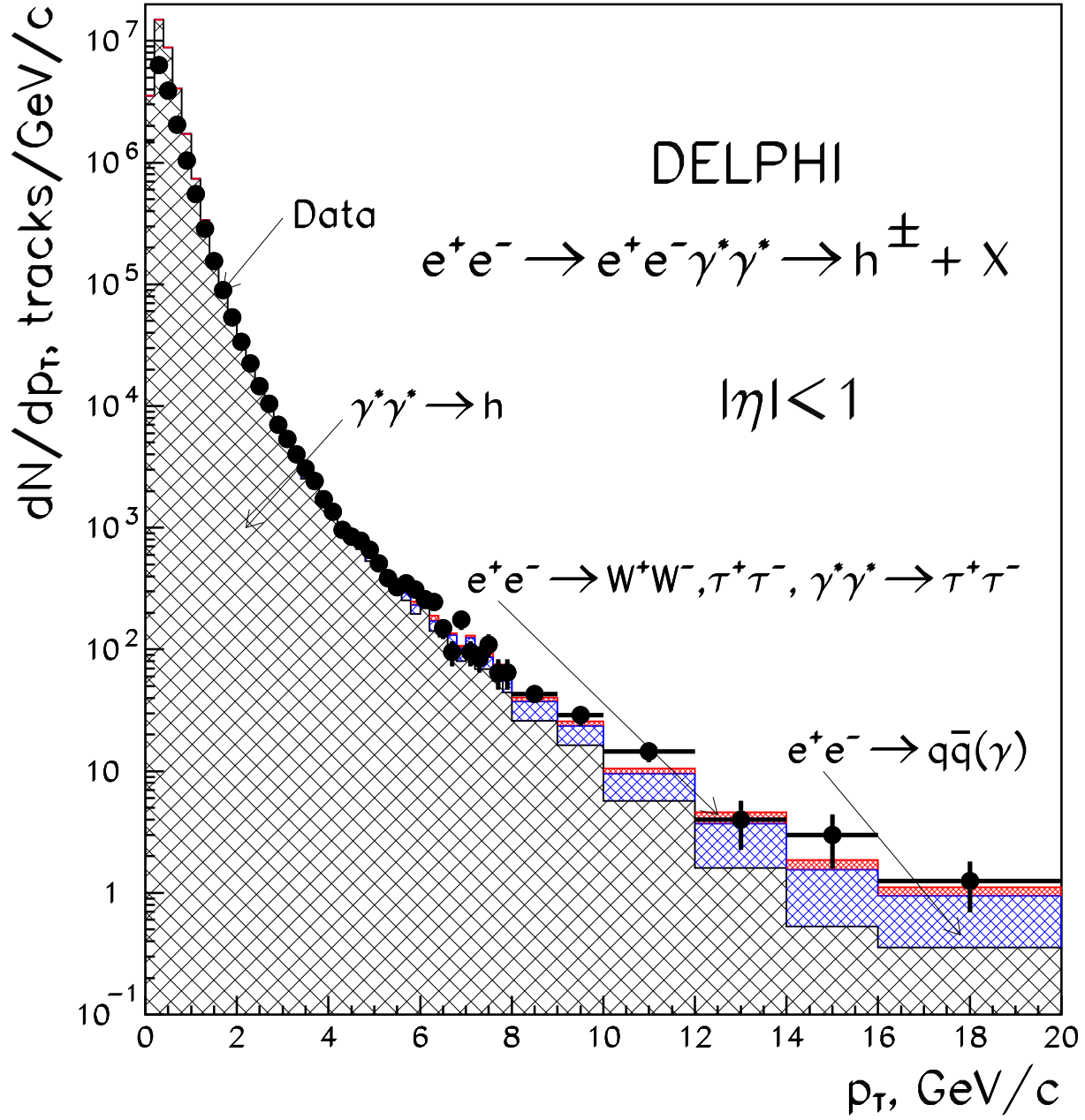


Figure 2: p_T distribution of charged particles of the selected sample of events, for $|\eta| < 1$ together with the Monte Carlo generated contributing processes: $\gamma^*\gamma^* \rightarrow \text{hadrons}$ (largest cross-hatching), $e^+e^- \rightarrow q\bar{q}(\gamma)$ (medium cross-hatching), $e^+e^- \rightarrow W^+W^-, \tau^+\tau^-$, $\gamma^*\gamma^* \rightarrow \tau^+\tau^-$ (small cross-hatching).

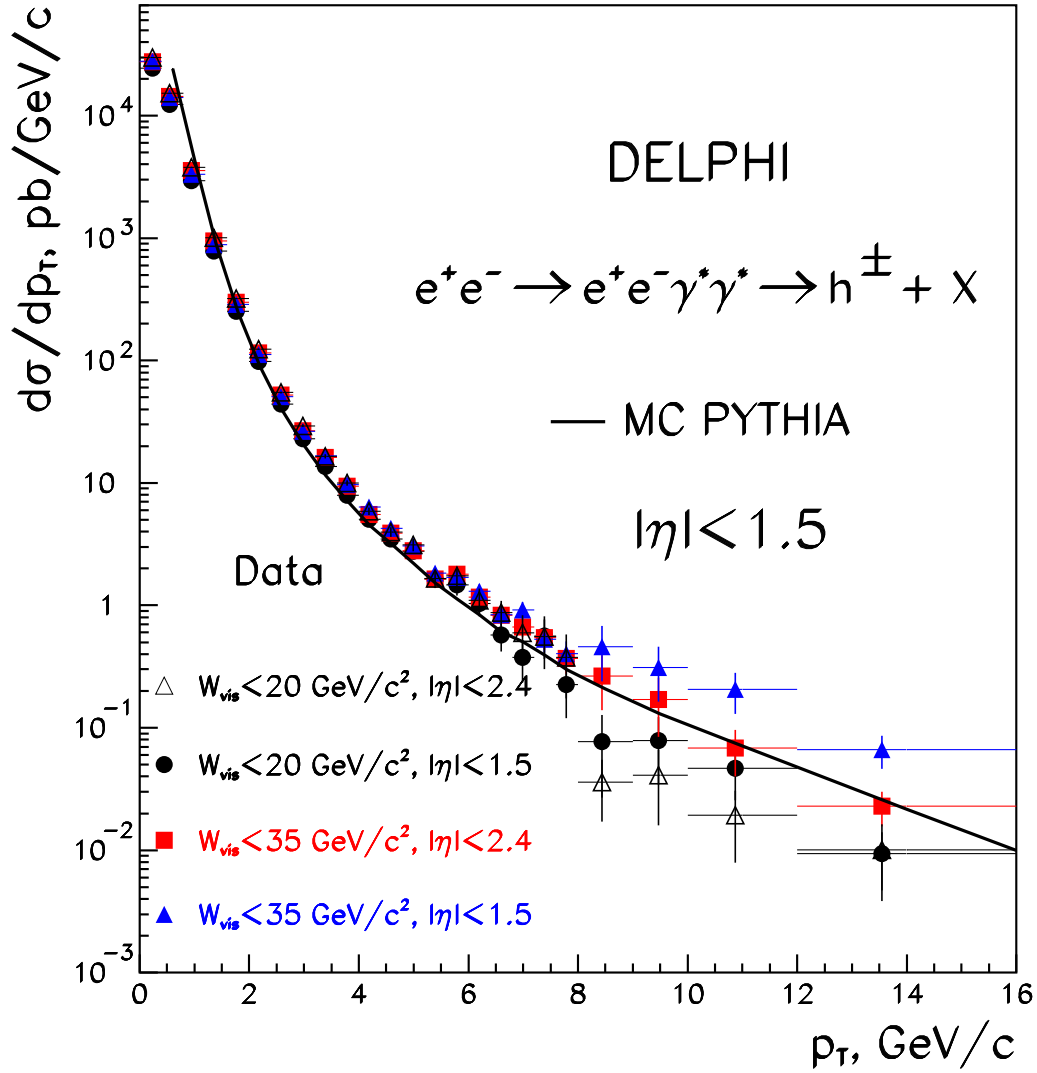


Figure 3: Differential inclusive $d\sigma/dp_T$ distributions of charged particles with $|\eta| < 1.5$, produced in $\gamma^*\gamma^*$ collisions, for different sets of initial selection criteria. (The lower limit of W_{vis} was $W_{vis} > 5 \text{ GeV}/c^2$). The data are background subtracted and corrected for detector inefficiency and selection cuts. The line is the corresponding PYTHIA prediction for $\gamma^*\gamma^* \rightarrow \text{hadrons}$.

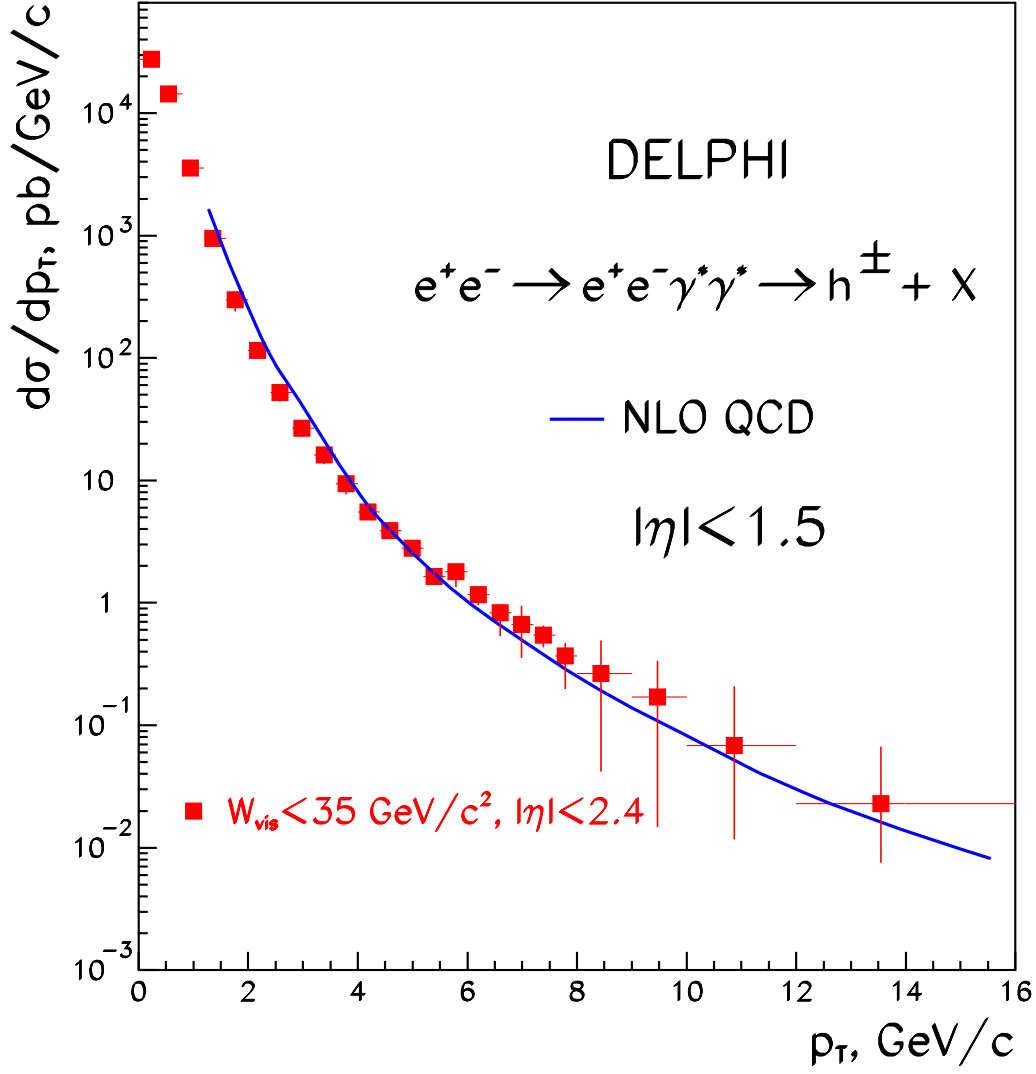


Figure 4: Differential inclusive $d\sigma/dp_T$ distribution of charged particles produced in $\gamma^*\gamma^*$ collisions for $|\eta| < 1.5$ and $5 \text{ GeV}/c^2 < W_{vis} < 35 \text{ GeV}/c^2$. The original data sample used to extract this cross section included tracks with $10^\circ < \theta < 170^\circ$ ($|\eta| < 2.4$). The data are shown as points with statistical + systematical error bars. They are background subtracted and corrected for detector inefficiency and selection cuts. The line is the NLO QCD prediction of [13] for $\gamma^*\gamma^* \rightarrow \text{hadrons}$.

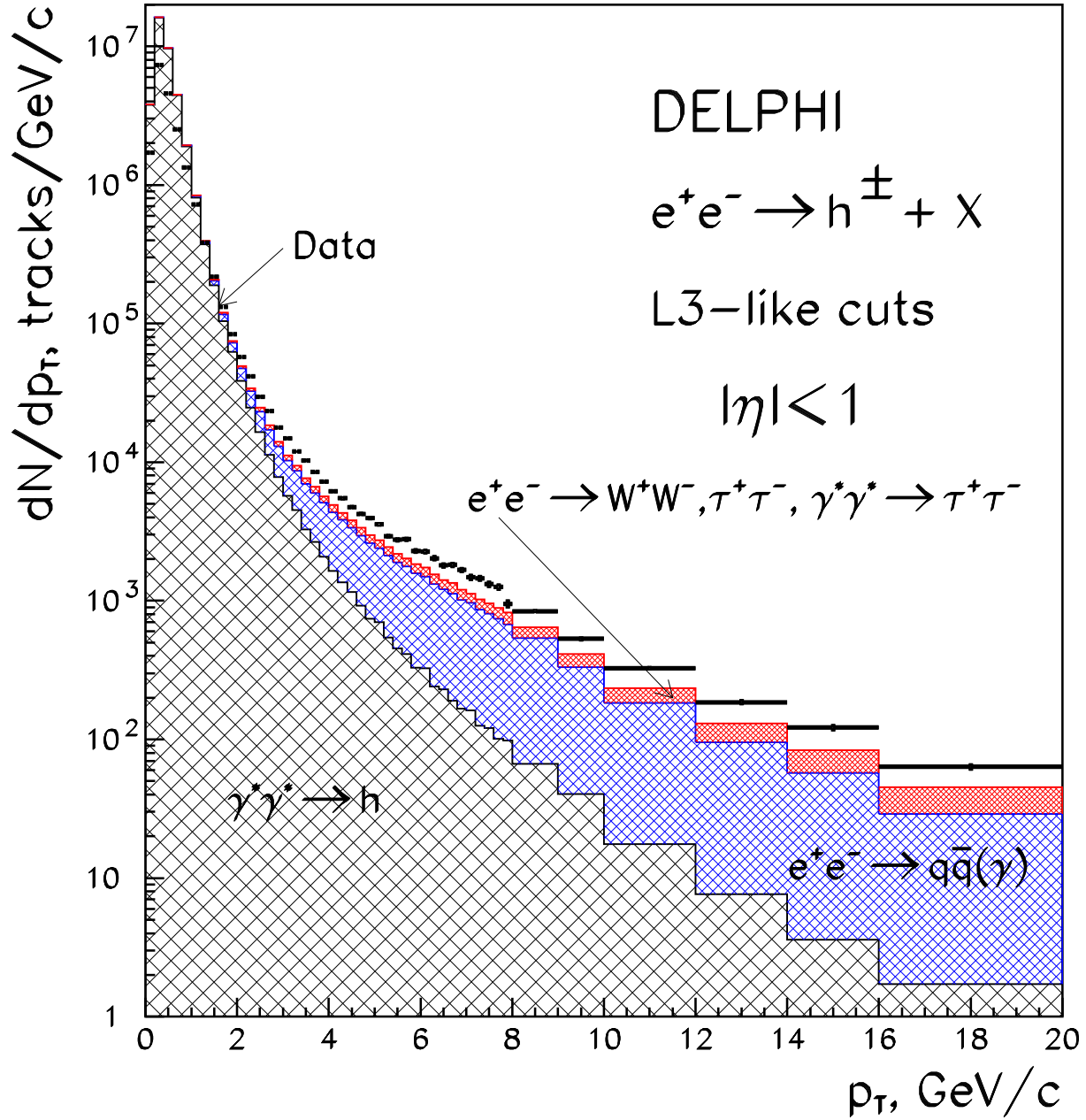


Figure 5: p_T distribution of charged particles of the event sample after application of the “L3-like” selection criteria, for $|\eta| < 1$ and $5 \text{ GeV}/c^2 < W_{vis} < 78 \text{ GeV}/c^2$, together with the Monte Carlo generated contributing processes: $\gamma^*\gamma^* \rightarrow \text{hadrons}$ (largest cross-hatching), $e^+e^- \rightarrow q\bar{q}(\gamma)$ (medium cross-hatching), $e^+e^- \rightarrow W^+W^-, \tau^+\tau^-, \gamma^*\gamma^* \rightarrow \tau^+\tau^-$ (small cross-hatching).